The effect of climate change on runoff from two watersheds in Iceland

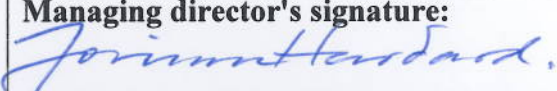Bergur Einarsson
Sveinbjörn Jónsson

Veðurstofa
Íslands

The effect of climate change on runoff from two watersheds in Iceland

Bergur Einarsson, Icelandic Meteorological Office
Sveinbjörn Jónsson, Icelandic Meteorological Office

Keypage

Veðurstofa
Íslands

Report no.: VÍ 2010-016	Date.: December 2010	ISSN: 1670-8261	Public ☒ Restricted ☐ Provision:

Report title / including subtitle	Number of copies:
The effect of climate change on runoff from two watersheds in Iceland	20
	Pages: 34

Authors: Bergur Einarsson and Sveinbjörn Jónsson	Managing director Jórunn Harðardóttir
	Project manager: Jórunn Harðardóttir

Project phase: Final report	Project number: 5811-0-0004

Report contracted for:

National Energy Authority / The project "Loftslagsbreytingar og áhrif þeirra á orkukerfi og samgöngur" (LOKS) / The Climate and Energy Systems project (CES)

Prepared in cooperation with:

Summary:

See abstract at beginning of report.

Keywords: Hydrological modelling, groundwater modelling, runoff scenarios, hydrological impact of climate changes, the hydrological model WaSiM, the CES project, Austari-Jökulsá, vhm 144, Sandá í Þistilfirði, vhm 26.	Managing director's signature: *Jórunn Harðardóttir,* Project manager's signature:
	Reviewed by: Philippe Crochet, Tómas Jóhannesson, SG

Contents

Figures

Tables

1 Abstract

In order to investigate the effect of climate change on the hydrological regime in Iceland, future projections of river discharge were made for two watersheds with the WaSiM hydrological model. The projections were made for the period 2021–2050 and compared with the reference period 1961–1990. The runoff projections are based on thirteen different climate scenarios. Monthly δ-changes, based on the climate scenarios, applied repeatedly to selected base years are used to construct the future climate input for the hydrological model. This methodology preserves the internal climate variability of the climate model runs.

The selected watersheds have different hydrological properties and climate characteristics. Sandá í Þistilfirði, vhm 26, is located close to the coast in the north-eastern part of Iceland and Austari-Jökulsá, vhm 144, is located in the northern part of the central highland with a 10% glacier coverage. Average warming for both watersheds between the reference period and the scenario period is on the order of 2°C. A precipitation increase of 16% is projected for Austari-Jökulsá and an increase of 3% for Sandá í Þistilfirði.

During the reference period 1961–1990, snow storage has a dominating effect on the discharge seasonality and snowmelt originated spring floods are the largest floods of the year for both watersheds.

Compared with the reference period, the magnitude of spring floods is predicted to decrease in 2021–2050 and they will appear earlier in the year. The timing of maximum snow melting is predicted to be about a month earlier for both watersheds and the magnitude of the mean yearly maximum snowmelt is predicted to decrease by 5–70%. The time with considerable snow cover is predicted to diminish from 7 months to 3–5 months per year depending on watershed. Mean yearly maximum snow thickness decreases by 0–80%.

Winter flow is predicted to increase on average due to a higher number of melt events at relatively high and flat heath areas of the watersheds. For Sandá í Þistilfirði, vhm 26, the snowmelt generated spring/summer discharge peak largely disappears and the seasonal discharge becomes more evenly distributed with higher winter discharge.

For Austari-Jökulsá, vhm 144, runoff from the glacier will increase substantially due to increased snow and ice melting. The share of glacier originated runoff in the total annual volume is predicted to increase from 20% to 25–30% and the duration of glacier runoff is predicted to increase by nearly two months, reaching further into the spring and autumn. The increase of annual glacier melt, assuming unchanged glacier geometry, is predicted to be in the range from 75–150% depending on scenario. This leads to a late summer discharge maximum caused by increased glacier runoff. The discharge peaks caused by snowmelt and glacier melt will become more distinct and appear as two separate summer maxima with the one caused by glacier melt the largest runoff peak of the year.

Compared to the period 1961–1990, a warming of about 1°C has already been observed for both watersheds during the period 2000–2009, causing considerable discharge changes in the same direction as the predicted future changes.

2 Introduction

Increased concentration of greenhouse gases in the atmosphere is predicted to lead to changed climate (IPCC, 2007). These changes will affect the hydrological regime as it is to large extent dependent on climatically controlled factors. The expected changes in the hydrological regime need to be estimated as it will be necessary to adapt to these changes. Increased temperature has been shown to cause changes in the storage of snow, in the magnitude of snowmelt floods and their timing along with changes in evaporation and major changes in glacier melting and thereby in the discharge of glacier-fed rivers. These changes will affect the hydropower industry, transportation and numbers of other sectors (Bergström *et al.*, 2007).

The consequences of climate change for the Nordic energy sector, in particular for the utilization of renewable energy sources, have been investigated in several collaborative Nordic research projects, of which the most recent is Climate and Energy Systems, (CES, 2007–2011), financed by The Nordic Energy Research and the Nordic energy sector (Snorrason & Harðardóttir, 2008). An Icelandic research project "Loftslagsbreytingar og áhrif þeirra á orkukerfi og samgöngur", (LOKS, 2008–2011) with a similar focus is working in parallel with the Nordic project.

The focus of one of the working groups in the CES project is on hydropower and hydrological modelling. One of the tasks of the Icelandic part of that workgroup was to improve the application of the hydrological model WaSiM in Iceland by: i) improving the representation of groundwater by activating the model's groundwater module; ii) improving the representation of seasonal changes in the Hamon evapotranspiration scheme; and iii) by applying glacier melt parameters calibrated by mass balance measurements instead of river discharge data. The National Energy Authority has supported this work with contracts on hydrological modelling and groundwater research. Further description of these improvements is given in Einarsson & Jónsson, (2010).

After these improvements had been implemented the model was used to make a future projection of discharge in Iceland for the period of 2021–2050. Two watersheds with different hydrological properties and climate characteristics were used. Sandá í Þistilfirði, vhm 26, located close to the coast in the north-eastern part of Iceland and Austari-Jökulsá, vhm 144, located in the northern part of the central highland with a 10% glacier coverage. The location of the watersheds (and the two subcatchments of vhm 144, vhm 269 and vhm 167) is shown on Figure 1.
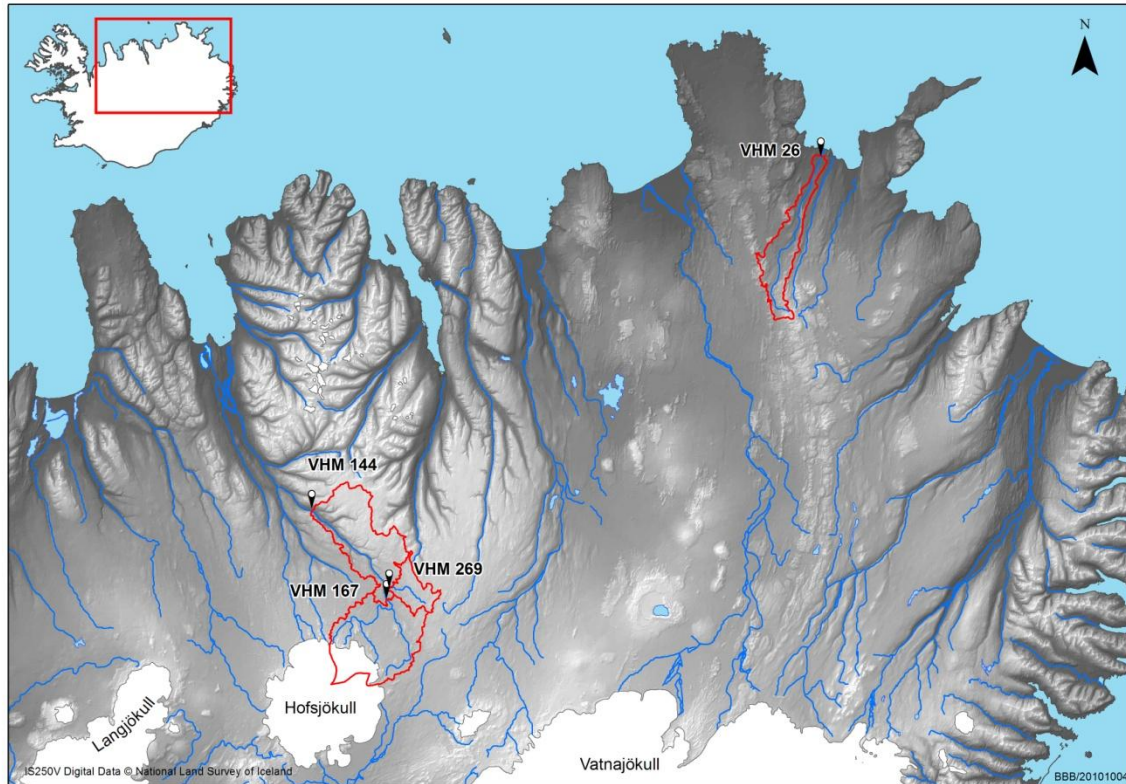
Figure 1. Location of the partly glacier covered watershed Austari-Jökulsá, vhm 144 (and its subcatchments vhm 167 and vhm 269) and the non-glacier covered watershed Sandá í Þistilfirði, vhm 26.

The WaSiM model (Jasper *et al.*, 2002; Jasper & Kaufmann, 2003) was first set up and calibrated in Iceland during the Nordic research project, Climate and Energy (CE) (Fenger, 2007), and the Icelandic sister project "Veðurfar og Orka" (VO) (Jóhannesson *et al.*, 2007). The model has been used to make a runoff map for Iceland for the period 1961–1990 and a future projection of runoff for the decades 2071–2100 (Jónsdóttir, 2008).

The calculation of a future hydrological prediction is described in Sections 3 and 4. The main results are then described in Section 5 and discussed and interpreted in Section 6.

9

3 Methods

WaSiM is a physically-based distributed hydrological model that has been used in recent years in Iceland and has proven reliable for modelling of mountainous areas with considerable snow accumulation (Kunstmann *et al.*, 2006).

The model offers various methods to calculate the different elements of the hydrological cycle depending on the availability of input data. For calculating evapotranspiration, the simple temperature-based Hamon approach was adopted. For calculating snowmelt, a temperature-wind index method was used where the effects on melting, of increased convectional thermal transport with increased wind speed are accounted for. Extended melt approach was used to account for melting on glaciers where the effects of radiation are added to a classic degree-day model. For infiltration, a methodology of Peschke, based on the approach of Green and Ampt, was used. To calculate the fluxes within the unsaturated soil zone, the Richards equation was used. The groundwater table was modelled in both the unsaturated zone module and the groundwater module. The coupling between both modules was done by a net boundary flux between the unsaturated zone and the groundwater (Schulla & Jasper, 2007).

Information on land use, soil type, elevation and other general properties of the watershed are given in static distributed grids while a number of parameters describing specific processes are adjusted to the properties of each watershed by comparison of modelled and measured discharge series.

In this study, the methodology used previously by Jónsdóttir (2008) is followed. Eleven parameters describing the unsaturated zone, snow accumulation, snow melt and groundwater flow were adjusted to fit each watershed. In addition, three parameters were adjusted for glacier covered areas. For the unsaturated zone, the following five parameters were adjusted: (1) Storage coefficient of direct runoff k_d; (2) storage coefficient of interflow k_i; (3) drainage density d; (4) the fraction of surface runoff from snowmelt; and (5) the recession constant k_{rec} for the decreasing saturated hydraulic conductivity with increasing depth. For the groundwater flow, adjusted parameters (6–7) are the hydraulic conductivity in the X and Y direction. The hydraulic conductivity is adjusted in distributed grids unlike other parameters that have one value for each sub-basin and are defined in the control file of the model. The four snow model parameters that were adjusted were (8) temperature threshold for rain/snow $T_{R/S}$, (9) temperature threshold for snow melt T_0, (10) degree-day factor without wind consideration c_1, and (11) degree-day-factor with wind consideration c_2. The additional three parameters that were calibrated for the glacier-covered watershed describes specific storage coefficients for (12–14): ice, snow, and firn. Model parameters were adjusted manually until simulated and observed discharge series were in agreement.

The Nash-Sutcliffe coefficient R^2 and R^2_{log} were used to measure how well the simulated runoff fits the observed runoff. Both coefficients R^2 and R^2_{log} range for 1 to $-\infty$, where a perfect fit corresponds to 1. The coefficient R^2 emphasizes the fit of high flows and floods while R^2_{log} puts greater weight on how well low flows are simulated (Jónsdóttir, 2008).

For a more detailed model description see Schulla & Jasper (2007).

4 Data

4.1 Discharge data

Discharge series from two watersheds are used in this study. These are the watershed corresponding to water-level gauge vhm 144 by Skatastaðir in the river Austari-Jökulsá and the watershed corresponding to gauge vhm 26 by Sandárfoss in the river Sandá í Þistilfirði. Discharge rating curves, relating water level to discharge, are available for both of these water-level gauges. Discharge series are therefore available for both gauges from the time of their setup to date. The gauge in Austari-Jökulsá, vhm 144, was built in 1970 while the one in Sandá í Þistilfirði, vhm 26, was built in 1965 (Icelandic Meteorological Office, 2010a; Icelandic Meteorological Office, 2010b). Those discharge series are not fully complete both because of instrument breakdown and ice interference. These data gaps in discharge are usually interpolated by estimation for most common use of these data, but all interpolated data are filtered out in this study.

The watershed of Austari-Jökulsá, vhm 144, was selected for studying because of its extensive glacier cover (10%). The area of the watershed is 1024 km^2 and it has had an average annual discharge of about 39 m^3/s for the last 37 years (Icelandic Meteorological Office, 2010a). The watershed is situated in the central highland and is highly elevated for an Icelandic watershed, the elevation profile of the watershed is shown on Figure 2. Apart from the glacier, the most important part of the watershed in terms of the hydrology is a large relatively flat heathen area. The spring floods are the most pronounced part of the mean annual hydrological variation, but the late summer glacier-peak is also pronounced.

Sandá í Þistilfirði, vhm 26, has a smaller watershed of only 268 km^2 and was selected as a typical direct runoff river. The watershed is at a lower elevation than the watershed of Austari-Jökulsá, vhm 144, and it is closer to the ocean. The elevation distribution of the watershed is shown on Figure 2. As for the watershed of Austari-Jökulsá and most watersheds in Iceland (Rist, 1990), the spring flood peak is most pronounced in the annual hydrological variation. The mean 33 year discharge average for Sandá í Þistilfirði is about 13.5 m^3/s (Icelandic Meteorological Office, 2010b).
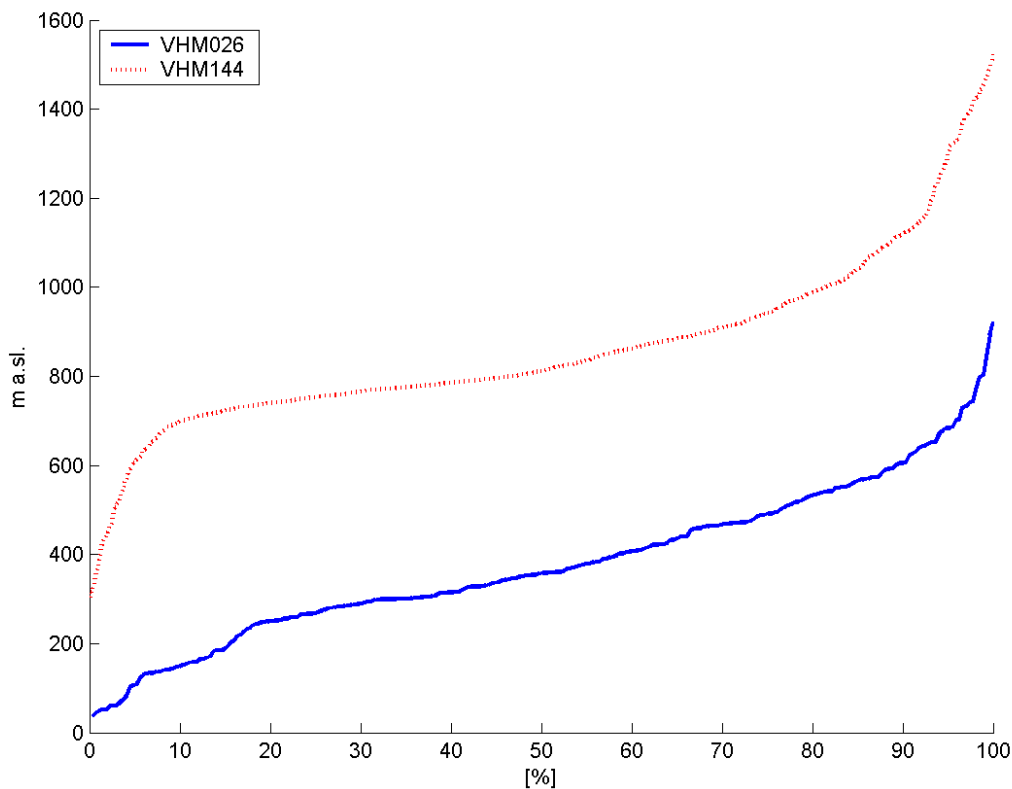
Figure 2. Elevation distribution for Sandá í Þistilfirði (vhm 26, blue curve) and Austari-Jökulsá (vhm 144, red broken curve).

4.2 Meteorological data

Information about precipitation, temperature, wind and incoming shortwave solar radiation are needed as input for the hydrological modelling. For this study, data from the meteorological PSU/NCAR MM5 numerical weather model were used (Grell *et al.*, 1994; Rögnvaldsson *et al.*, 2007). These data were calculated on an 8x8 km grid and exported into grids usable for input into WaSiM. The data are further interpolated onto a 1x1 grid within WaSiM.

During the calibration of Sandá í Þistilfirði, snow melt was observed to start unreasonably too early independently of parameterization, and most of the winter snow pack was melted already in January leaving no snow to be melted during April as observed. This led to suspicion about the quality of the simulated temperature data for this watershed. For this reason, it was decided to compare the MM5 temperature to a gridded temperature data set estimated by Crochet and Jóhannesson (2011), from the manual observation network. These gridded temperature data are calculated with a tension-spline interpolation after correction for elevation, using a 1-km Digital Terrain Model and a constant lapse-rate of -6.5°C/km. The result of this comparison showed that the MM5 temperature data were systematically higher than observed as shown in Table 1 and on Figure 3. This is in agreement with an earlier comparison of MM5 temperature data with spatial interpolated observed temperatures. In Jóhannesson *et al.* (2007), the MM5 temperature was found to be 0.9°C warmer on the average for the period 1961–1990.

12

Month	Jan	Feb	Mar	Apr	May	Jun	Jul	Aug	Sep	Oct	Nov	Dec	Win	Sum	Year
Mean MM5 [C°]	-3.2	-3.1	-3.2	-1.6	1.8	5.8	8	7.5	4.3	1.2	-1.7	-3.1	-3.1	7.1	1.1
Mean obs. [C°]	-4.3	-4.1	-3.8	-1.6	1.8	5.4	7.4	7.1	3.9	0.5	-2.5	-4.1	-4.1	6.6	0.5
Difference	1.1	1.0	0.6	0.0	0.0	0.4	0.6	0.4	0.4	0.7	0.8	1.0	1.0	0.5	0.6
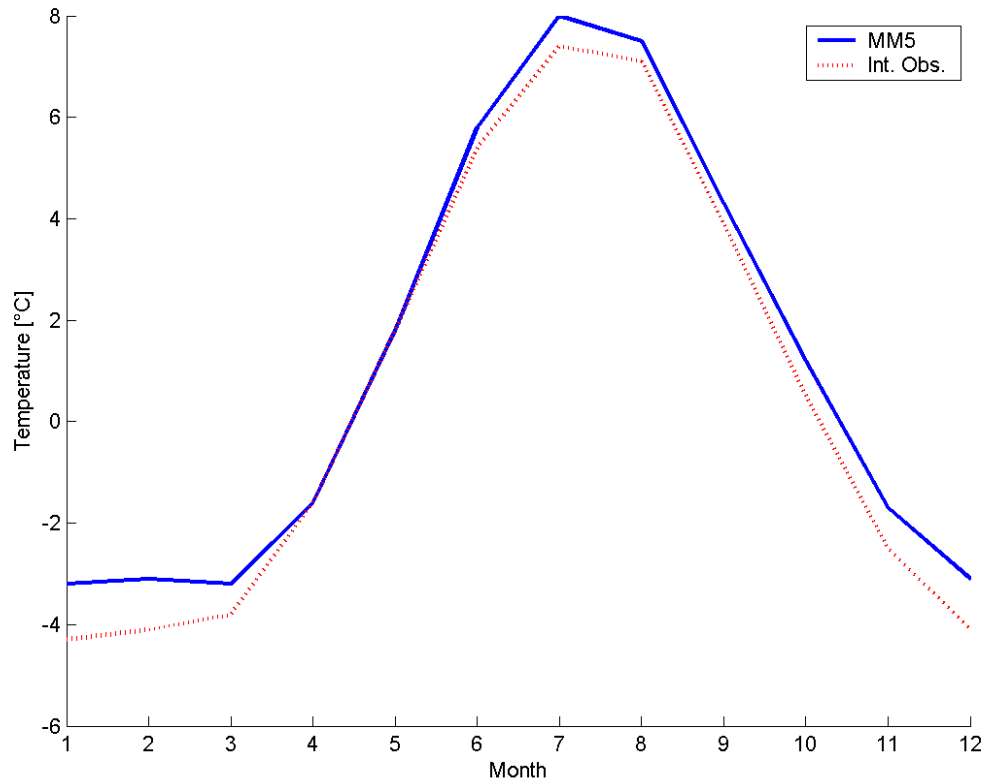
Figure 3. Comparison of mean yearly temperature 1961–2005 for Sandá í Þistilfirði (vhm 26); an interpolation of manual observation is shown with a broken red curve and MM5 temperature is shown in blue.

Due to this systematic difference the MM5 temperatures data were corrected to fit the mean monthly gridded values, see Table 1.

No suspicion about the quality of the MM5 temperature data arose when calibrating the Austari-Jökulsá watershed; but when comparing the MM5 temperatures to the interpolated ones, a similar difference was observed. The MM5 temperatures were also systematically higher than observations for the winter months as shown in Table 1 and Figure 4.

The high elevation gradient for the lowest areas of the Austari-Jökulsá watershed (see Figure 2) reduces the effect of this temperature bias. The difference is most pronounced for the cold winter months November to March when melting only takes place in warm events and then generally only on the lower part of the watershed. As the elevation gradient for the lower part is high the temperature bias in the MM5 data will only cause the addition of a narrow elevation band with small area reaching above the melt threshold.

Added unrealistic melt will therefore be small. The effects on runoff are therefore much less pronounced than for Sandá í Þistilfirði and were therefore not noticed during the calibration. This bias in the modelled temperature data should nevertheless have been corrected but due to time constraints and since this was not noticed until after the calibration of the watershed this was not done.

Table 2. Mean monthly temperature for Austari-Jökulsá (vhm 144), 1961–2005.

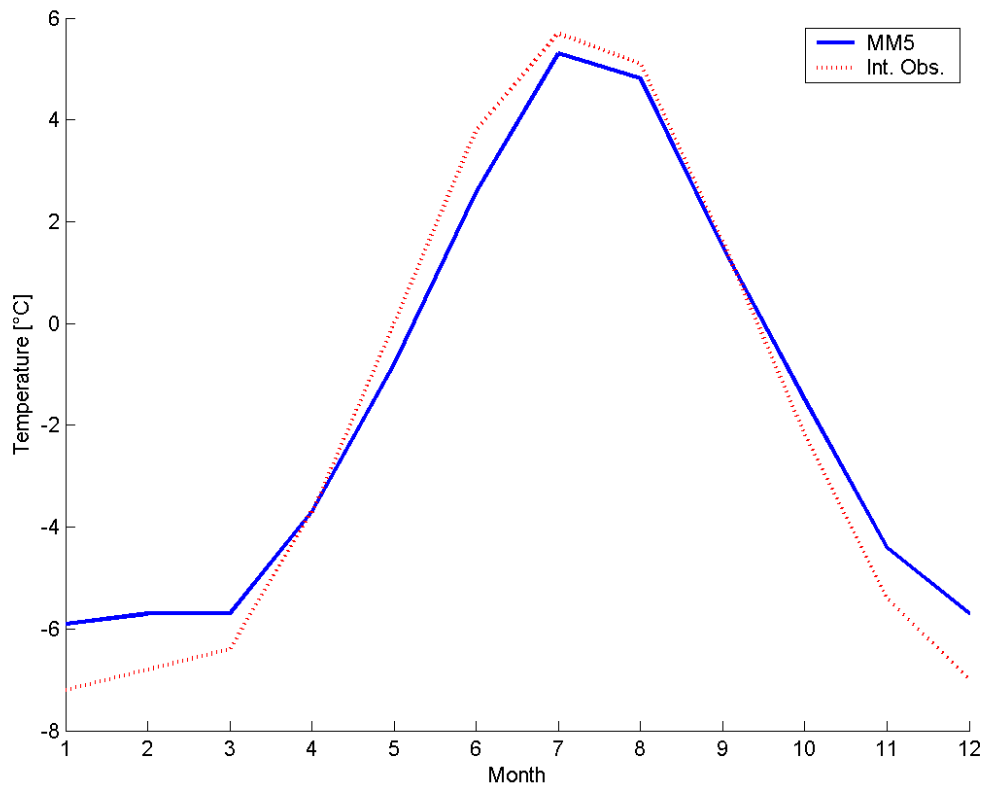| Month	Jan	Feb	Mar	Apr	May	Jun	Jul	Aug	Sep	Oct	Nov	Dec	Win	Sum	Year
Mean MM5 [C°]	-5.9	-5.7	-5.7	-3.7	-0.8	2.6	5.3	4.8	1.5	-1.5	-4.4	-5.7	-5.7	4.3	-1.5
Mean obs. [C°]	-7.2	-6.8	-6.4	-3.7	0	3.8	5.7	5.1	1.6	-2.2	-5.4	-7.0	-7.0	4.9	-1.8
Difference	1.3	1.1	0.7	0.0	-0.8	-1.2	-0.4	-0.3	-0.1	0.7	1.0	1.3	1.3	-0.6	0.3

Figure 4. Comparison of mean yearly temperature 1961–2005 for Austari-Jökulsá (vhm 144); an interpolation of manual observation is shown with a broken red curve and MM5 temperature is shown in blue.

4.3 Climate scenarios

The CES climate scenario group recommended three dynamically downscaled RCM scenarios (ECHAM5-r3/DMI-HIRHAM5, HadCM3/MetNo-HIRHAM, BCM/SMHI-RCA3). For Iceland, a more recent downscaling of the ECHAM5-r3 global model with the RCAO regional model (Döscher *et al.*, 2010) was used instead of the BCM/SMHI-RCA3 downscaling. The hydrological simulations in Iceland also made use of a data set of 10 global AOGCM climate change simulations based on the A1B emission scenario submitted by various institutions to the IPCC for its fourth assessment report (IPCC, 2007). These 10 GCMs were chosen from a larger IPCC data set of 22 GCMs based on their SAT (surface air temperature) performance compared with the ERA-40 reanalysis in the period 1958–1998 in an area in the N-Atlantic encompassing Iceland and the surrounding ocean (Nawri & Björnsson, 2010).

The recent warming in Iceland has been particularly rapid, with a warming of ~1.25–2°C taking place at most weather stations in Iceland during the last 30 years. This rapid recent warming complicates the interpretation of climate change scenarios specifying a change in climate with respect to a past baseline period. The expected climate change during the next several decades with respect to the CES baseline period 1961–1990 depends crucially on how much of the rapid warming since the baseline period is viewed as a part of a deterministic warming trend and how much is viewed as a part of random climate variability. A temporary warming trend caused mainly by climate variability is likely to revert back to relatively cooler temperatures over a time period determined by the statistical autocorrelation of the temperature time-series.

There are many issues that need to be considered in the derivation of scenarios for short term climate change impact assessments. The most important are:

Type of scenario. Typical δ-change scenarios have various flaws. For example they do not preserve the variability from regional climate models, but only resample the internal variability of former climate used as base. Direct model output is, however, often difficult to use because of biases that make it unsuitable for hydrological modelling.

Baseline period. The climate of any past baseline period such as 1961–1990 or 1971–2000 is characterised by a particular realisation of natural variability which is unlikely to be repeated in the future. In most cases, the climate of a (past) baseline period in a particular GCM simulation is characterised by internal "natural" variability of the respective GCM which has nothing to do with the actual climate during the same period in the real world. Using differences with respect to such a past baseline period unnecessarily introduces substantial uncertainties about past climate into the δ-change scenario. The use of the baseline period as a reference for comparison with a possible future climate needs to be separated from the use of the baseline period in the derivation of a climate change scenario.

Recent climate changes. A scenario needs to merge smoothly with the recent past climate, taking into account the effect of recent climate change that may partly be of anthropogenic origin and also the substantial internal autocorrelation of the climate. Past climate is in principle known and there is no reason to let internal "natural" variability of climate model simulations, during already elapsed time periods, introduce uncertainty into climate change scenarios.

Seasonality of climate changes. The annual cycle has a substantial effect on many aspects of the water cycle. There is large uncertainty regarding modelled changes in the seasonality of many climate variables. Modelled changes in seasonality need to be

considered in detail and the deterministic component separated from the effects of random natural variability and, to the extent possible, model errors and biases.

Surface characteristics. The crude resolution of GCMs and some RCMs leads to an underestimate of the continentality of the climate at the location of some watersheds in Iceland. The model cells nearest to the watershed may contain large ocean areas that bring maritime effects far inland and into mountain areas where the climate is in reality to a large degree sheltered from maritime effects. It is particularly important to consider this problem when GCMs model results are directly used to derive climate change scenarios without downscaling.

Choice of climate models. There is considerable variation in the realism of different climate models regarding the present-day climate in particular regions of the globe. Climate models need to be evaluated to detect serious biases and obvious errors that may degrade the quality of any scenarios derived from them.

Internal consistency of climate variables. Hydrological simulations are based on several climate variables simultaneously. It is important that time-series of different climate variables in such modelling maintain their internal consistency when scenarios are derived. Precipitation has, for example, a tendency to fall on relatively warm days whereas cold periods have a tendency to be dry in some climate regions. It may be crucial to maintain such relationships in scenarios of future climate for simulations of future hydrological response to climate change to be meaningful.

Based on the above considerations, climate change scenarios for the hydrological modelling in Iceland where derived as follows (more details are given by Jóhannesson, 2010).

1. The choice of RCM and GCM models was based on the analysis of Nawri & Björnsson (2010) and on the recommendations of the CES scenario group. This resulted in a total of 13 scenarios, 3 RCM-based and 10 based on IPCC GCM simulations. The choice of the GCM models was based on their SAT performance for the present-day climate near Iceland as mentioned above.

2. For GCM-based scenarios, temperature change in the highland interior of Iceland, where the large ice caps are located, were increased by 25% based on the results of RCM downscaling (Nawri & Björnsson, 2010).

3. Expected values for temperature and precipitation in 2010 were estimated by statistical AR modelling, thereby taking into account the warming that has been observed in recent years as well as the inertia of the climate system so that the very high temperatures of the last few years have only a moderate effect on the derived expected values. These expected values are intended to represent the deterministic part of the recent variation in climate when short-term climate variations have been removed by the statistical analysis.

4. Scenarios of monthly mean temperature and accumulated precipitation where calculated from 2010 to the end of the climate simulation by fitting a least squares line to the monthly values simulated by the RCM or GCM from 2010 onwards and shifting the simulated time-series vertically so that the 2010 value of the least squares line matched the expected 2010 value based on the AR modelling of past climate. In this manner, the 1961–1990 CES baseline period was not directly used in the derivation of the future scenario. The CES baseline may nevertheless be used to express the scenario in terms of differences with respect to the baseline period when desired.

The trend analysis of future climate eliminates the direct use of a past baseline period in the derivation of the scenarios and provides a consistent match with the recent climate development. The statistical matching of the past climate observations with the trend lines of the future climate, furthermore, provides an implicit bias correction. This is important near Iceland because the RCM and GCM simulations showed great biases with respect to observations in this area and the simulations of past variations in the climate were also quite different from the actual climate development, particularly with respect to the overall cold temperatures of the period 1961–1990 and the magnitude of the warming of the last decades.

The climate scenarios used are constructed for a meteorological station close to each of the two watersheds studied. The ones used for Sandá Í Þistilfirði are constructed for the meteorological station at Raufarhöfn, which is located about 35 km north of watershed. The ones used for Austari-Jökulsá are constructed for the meteorological station at Hveravellir in central Iceland, which is located about 60 km south-west of the watershed.

Figure 5 shows the 13 scenarios for annual mean temperature at the meteorological station Hveravellir together with a temperature time-series from Stykkishólmur, western Iceland, that extends back to the early half of the 19th century. The left panel shows that, with the exception of the scenario based on the CSIRO_MK35 GCM model, the scenarios exhibit apparently random interannual to decadal variations, with a magnitude similar to past variations in the Stykkishólmur and Hveravellir records, superimposed on a general warming trend. The CSIRO_MK35 GCM model stands out with much greater interannual and decadal variations that appear to be substantially larger than past variations in temperature in spite of this model being one of the 10 models chosen from the set of 22 IPCC models with an overall realistic temperature performance in terms of bias and spatial variations in this area. One GCM model (MIUB_Echo_G) has somewhat smaller warming than the others, particularly near the end of the 21st century, whereas another (UKMO_HadCM3) indicates a greater rate of warming and comparatively large amplitude of interannual to decadal variations compared with the others. With the possible exception of the CSIRO_MK35 GCM model, this set of scenarios may provide an indication of the range of natural variability of the climate of the early 21st century as well as the magnitude of model uncertainties that may be expected in simulations with current GCM and RCM models. These simulations indicate a warming of close to 2°C near the end of the period 2021–2050 with respect to 1981–2000, about half of which has already taken place, and a warming of ~3–4°C by the end of the 21st century. Changes with respect to the CES baseline period 1961–1990 are very similar.
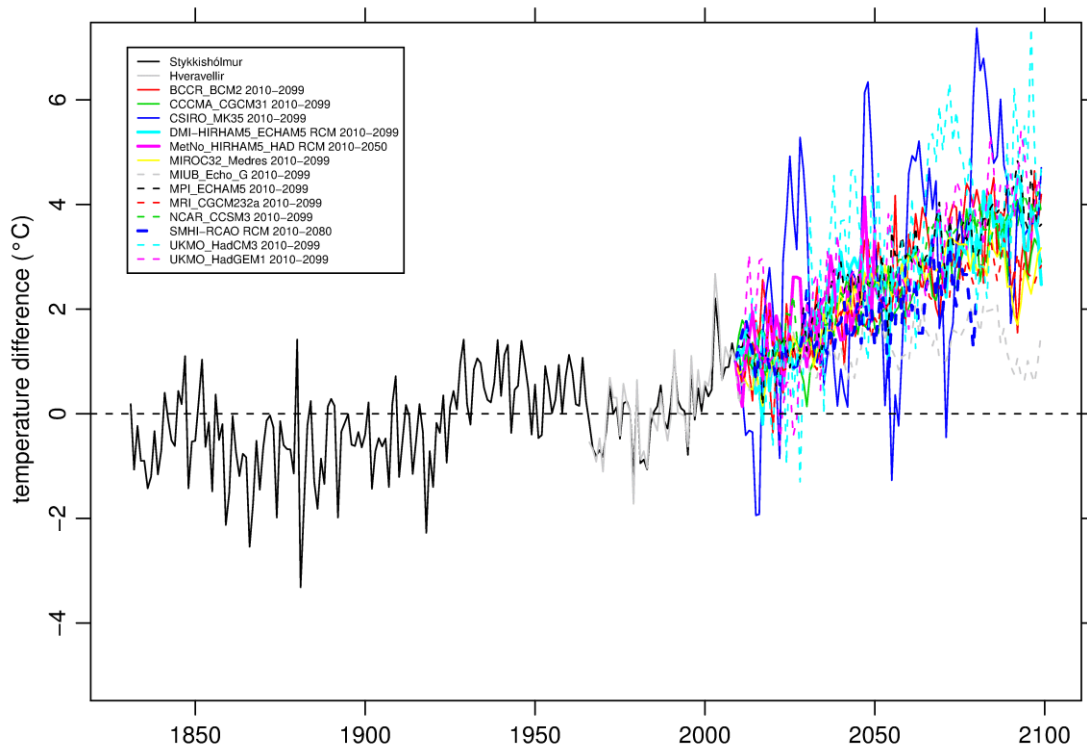
Figure 5. Future scenarios for annual mean temperature at Hveravellir, central Iceland. The longest temperature time-series from Iceland reconstructed for the Stykkishólmur meteorological station back to 1831 is also shown. All 13 scenarios are shown (see text for explanations). The figures show the difference of the mean annual temperature of glaciological years (starting in October of the previous year and ending in September of the respective year) with respect to the average of the period 1981–2000.

An analysis of the seasonality of the temperature changes shows that the warming is somewhat greater during the autumn and winter compared with the spring and summer. This is similar as is found in earlier analyses of future climate change in Iceland (Björnsson *et al.*, 2008).

Precipitation changes were found to be dominated by the simulated "natural" climate variability. For some stations, including Hveravellir, the AR statistical analysis of recent changes indicated an increase in precipitation in the last few decades, but for others this was not the case. Typically, a slow increase of ~5–10% was found during the 21st century without a consistent seasonal variation.

Internal consistency between different meteorological variables must be kept within climate scenarios as mentioned above. To keep the internal consistency, the climate scenarios were based on meteorological data from a base year that is close to the mean of the baseline period 1981–2000 in their climatic characteristics. To account for changes in temperature and precipitation, the monthly δ-changes, with respect to the period 1981–2000, for each future year are applied repeatedly to the base year data. By this method, monthly variability from the climate scenario runs is preserved along with the internal consistency between meteorological variables from the selected base year.

This methodology is not without flaws and this affects the results. The day to day climate characteristics of the scenarios will be dominated by the climate characteristics of the selected base year and this affects analyses of changed flood behaviour and timing as discussed further below. None of the selected years is a perfect fit to the 1981–2000 means, but care is taken to check that they are not outliers in any way. The runoff modelling depends therefore on the selection of base year. Averages of outputs from runoff calculations based on the three different base years are used for final results to minimize these effects.

The base years are selected from the period of available meteorological data which is 1961–2005. The selection was based on a comparison of seasonal temperature, precipitation and discharge variation with the mean seasonal variation for 1981–2000 by using root mean square error to measure the deviation. Deviation of annual means from 1981–2000 means in temperature, precipitation and discharge is also used. Finally, visual inspection comparing the seasonal temperature, precipitation and discharge variation to the 1981–2000 means was used to confirm the selection. For Sandá í Þistilfirði the years 1962, 1989, and 2001 were selected and for Austari-Jökulsá 1975, 1977, and 1999 were selected.

Median, max and min changes of temperature and precipitation predicted by the thirteen different climate scenarios for each of the meteorological station used is given in Table 3. The values are based on comparison for mean values for 1961–1990 and mean values for each scenario for 2021–2050.

Table 3. Difference in temperature and precipitation between the reference period and the climate scenarios.

	ΔT_{median} [°C]	ΔP_{median} [%]	ΔT_{max} [°C]	ΔP_{max} [%]	ΔT_{min} [°C]	ΔP_{min} [%]
Raufarhöfn	2.0	3	2.8	7	1.4	-1
Hveravellir	1.8	20	2.6	25	1.2	15

5 Results

Modelled average discharge series for the periods 1961–1990 and 2000–2009 along with average predicted discharge for 2021–2050 based on the thirteen above mentioned climate scenarios is shown on: Figure 6 for Sandá í Þistilfirði, vhm 26, and on Figure 7 for Austari-Jökulsá, vhm 144. Similarly modelled snowmelt for the periods 1961–1990 and 2000–2009 along with predicted snowmelt for 2021–2050 based on the thirteen above mentioned climate scenarios is shown on Figure 9 for Sandá í Þistilfirði and on Figure 10 for Austari-Jökulsá. The modelled discharge from the glacier covered part of Austari-Jökulsá for the periods 1961–1990 and 2000–2009 along with predicted discharge for the period 2021–2050 is in addition shown on Figure 8. The modelled snow storage for the periods 1961–1990 and 2000–2009 along with predicted snow storage for the period 2021–2050 is finally shown on Figure 11 for Sandá í Þistilfirði and on Figure 12 for Austari-Jökulsá.

The magnitude of spring floods in Sandá í Þistilfirði is predicted to decrease for all scenarios compared with both 1961–1990 and for 2000–2009, see Figure 6. The magnitude of spring floods in Austari-Jökulsá is predicted to decrease for all scenarios

except one compared to 1961–1990 while the prediction envelopes the mean magnitude of 2000–2009, see Figure 7.
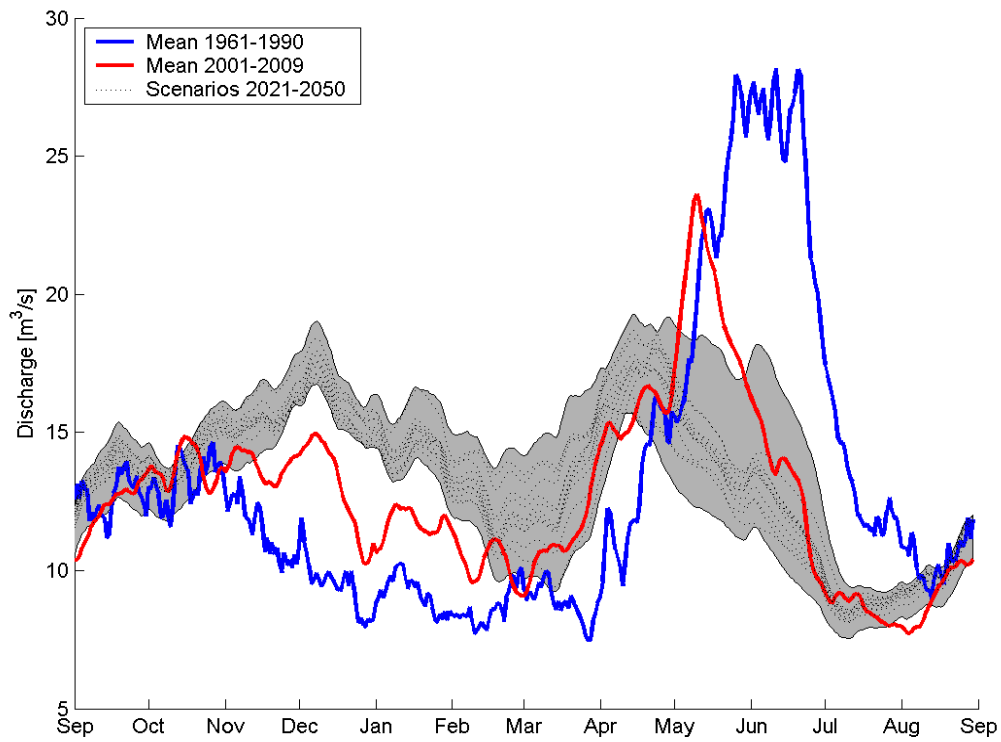
Winter flow is predicted to increase on the average due to a higher number of melt events on the relatively high and flat heath areas of both Austari Jökuslá and Sandá í Þistilfirði. For Sandá í Þistilfirði the snowmelt generated spring/summer discharge peak is strongly reduced (see Figure 9) and the seasonal discharge becomes more evenly distributed with increased winter discharge, see Figure 6. For Austari-Jökulsá, increased snow melt during winter causes a peak in average flow during late winter, February to March, see Figure 7 and Figure 10. This winter peak might though be unrealistic due to large winter floods during this period in two of the base years enhanced by the predicted warming.

For Austari Jökuslá, vhm 144, runoff from the glacier will increase substantially due to increased snow and ice melting, see Figure 7. The share of glacier originated runoff in the total annual volume is predicted to increase from 20% to 25–30% and the duration of glacier runoff is predicted to increase by nearly two months, reaching further into the spring and autumn, see Figure 8. The increase of annual glacier melt, assuming unchanged glacier geometry, is predicted to be in the range from 75–150% depending on scenario, see Table 4. This leads to a late summer discharge maximum caused by increased glacier runoff. The discharge peaks caused by snowmelt and glacier melt will become more distinct and appear as two separate summer maxima with the one caused by glacier melt, the largest runoff peak of the year, see Figure 7.

The timing of maximum snow melting is predicted to be about a month earlier for both watersheds and the magnitude of the mean yearly maximum snowmelt is predicted to decrease by 5–70%, see Figure 9, Figure 10 and Table 4. The time with considerable snow cover is predicted to diminish from 7 months to 3–5 months per year depending on watershed and the mean yearly maximum snow thickness decreases by 0–80%. The timing of maximum snow storage is not predicted to change drastically except for the warmest scenarios for Austari-Jökulsá where the timing of maximum snow storage is moved from April to February and January, see Figure 11 and Figure 12.

Table 4. Predicted quantitative changes from 1961–1990 to 2021–2050.

	Precipitation change	Mean decrease of yearly max snowmelt	Mean decrease of yearly max snow thickness	Change in share of glacier originated runoff	Change in annual glacier melt
Austari-Jökulsá, vhm 144	+16%	5%−70%	0%−65%	10%	75−150%
Sandá í Þistilfirði, vhm 26	+3%	45%−70%	41%−80%	–	–

Figure 6. Mean discharge seasonality for scenario runs compared with the period 1961–1990 (shown in blue) and the more recent period 2000–2009 (shown in red) for Sandá í Þistilfirði (vhm 26). Discharge seasonality for each scenario for 2021–2050 is shown with grey broken curves and the area between maximum and minimum predicted discharge is colored grey.
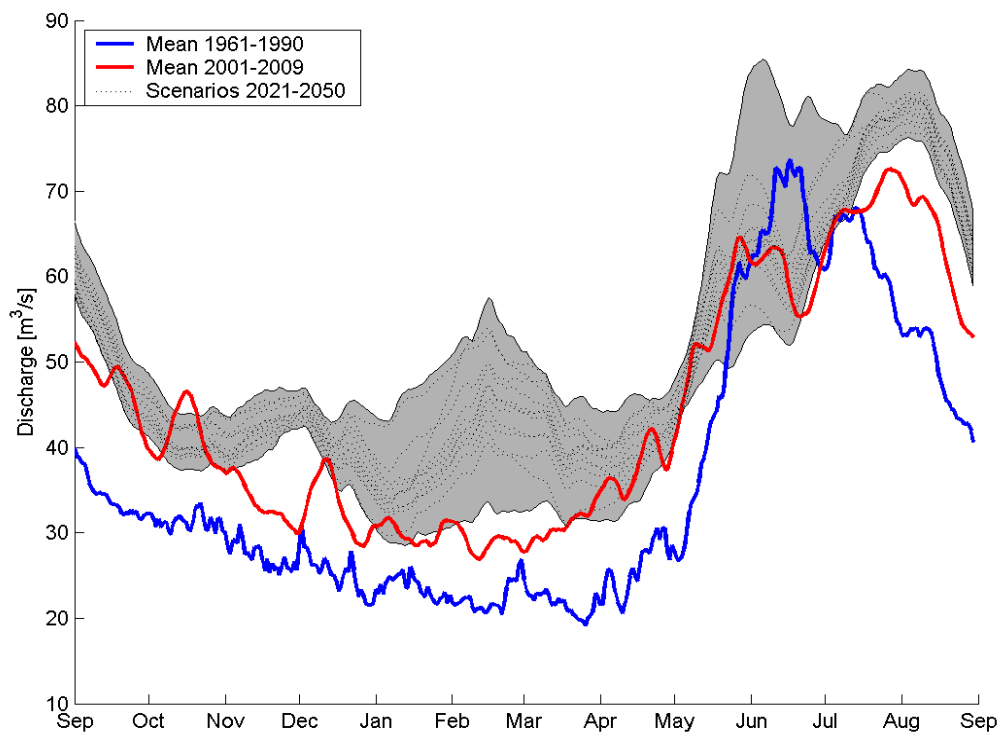
Figure 7. Mean discharge seasonality for scenario runs compared with the period 1961–1990 (shown in blue) and the more recent period 2000–2009 (shown in red) for Austari-Jökulsá (vhm 144). Discharge seasonality for each scenario for 2021–2050 is shown with grey broken curves and the area between maximum and minimum predicted discharge is colored grey.

Figure 8. Mean glacier originated discharge seasonality for scenario runs compared with the period 1961–1990 (shown in blue) and the more recent period 2000–2009 (shown in red) for Austari-Jökulsá (vhm 144). Discharge seasonality for each scenario for 2021–2050 is shown with grey broken curves and the area between maximum and minimum predicted discharge is colored grey.

Figure 9. Mean snowmelt seasonality for scenario runs compared with the period 1961–1990 (shown in blue) and the more recent period 2000–2009 (shown in red) for Sandá í Þistilfirði (vhm 26). Snowmelt seasonality for each scenario for 2021–2050 is shown with grey broken curves and the area between maximum and minimum predicted snowmelt is colored grey.

Figure 10. Mean snowmelt seasonality for scenario runs compared with the period 1961–1990 (shown in blue) and the more recent period 2000–2009 (shown in red) for Austari-Jökulsá (vhm 144). Snowmelt seasonality for each scenario for 2021–2050 is shown with grey broken curves and the area between maximum and minimum predicted snowmelt is colored grey.
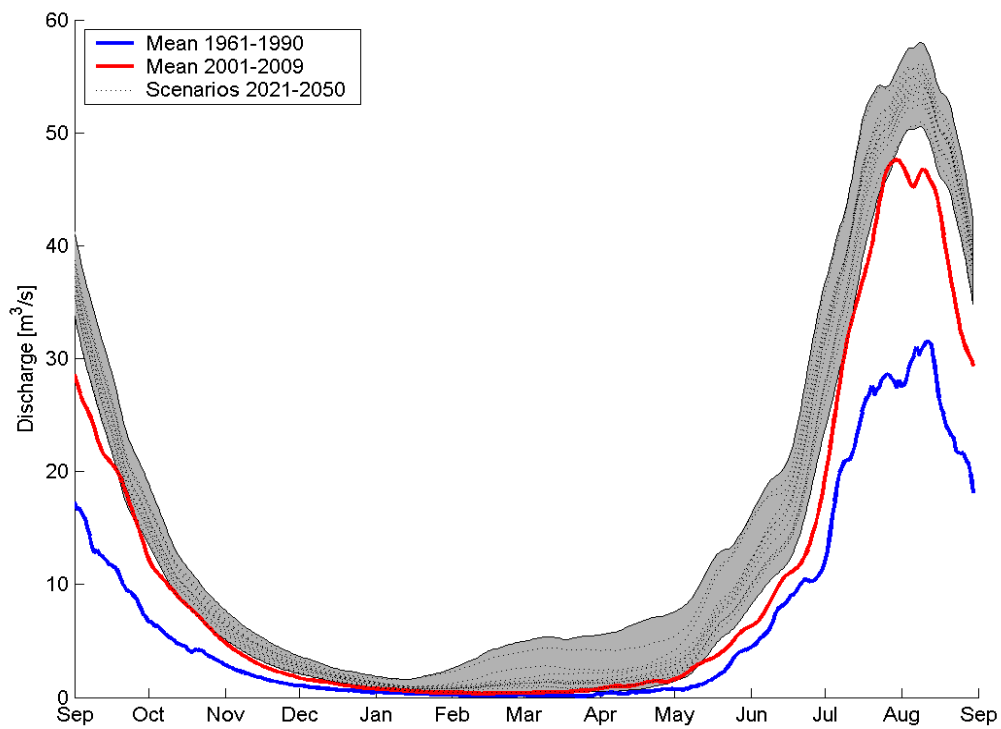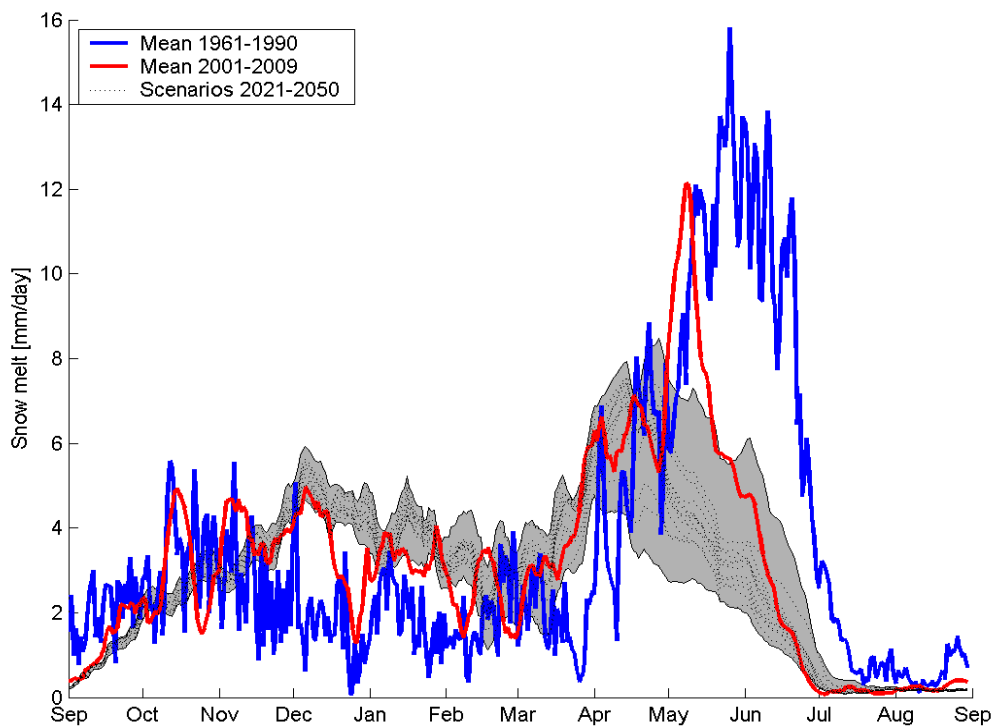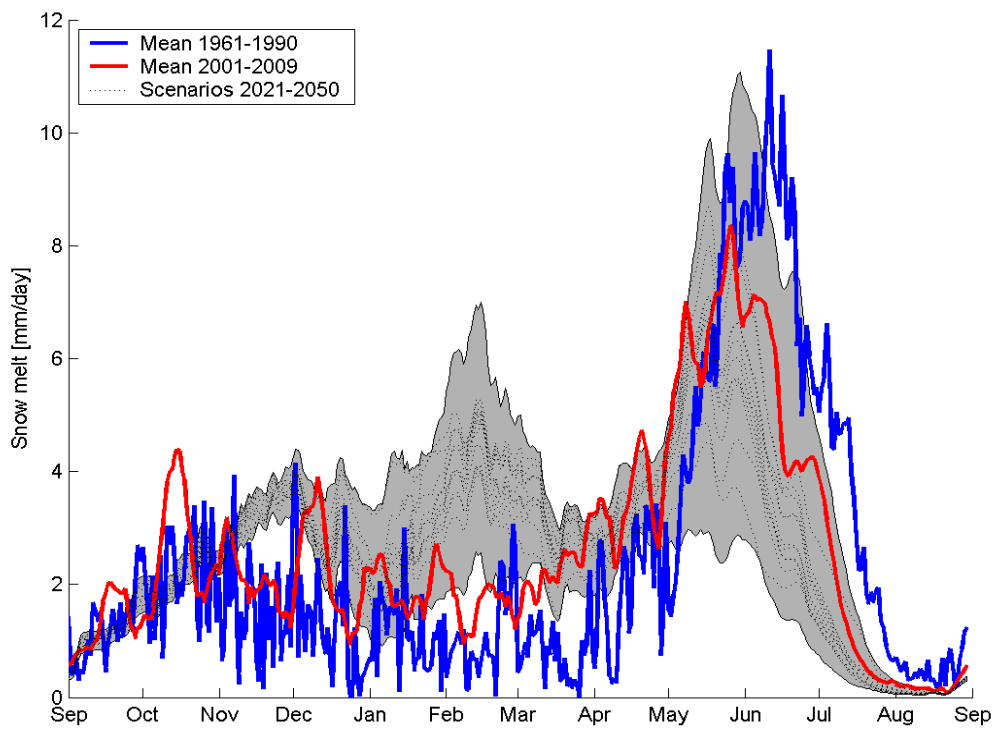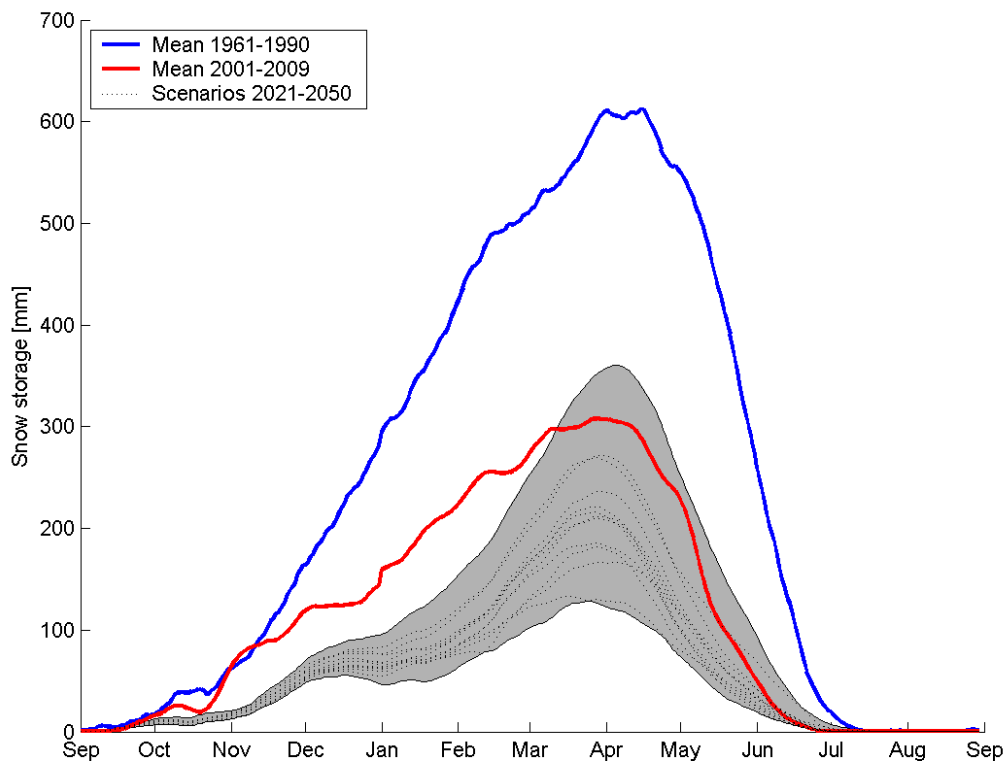
Figure 11. Mean snow storage seasonality for scenario runs compared with the period 1961–1990 (shown in blue) and the more recent period 2000–2009 (shown in red) for Sandá í Þistilfirði (vhm 26). Snow storage seasonality for each scenario for 2021–2050 is shown with grey broken curves and the area between maximum and minimum predicted snow storage is colored grey.

Figure 12. Mean snow storage seasonality for scenario runs compared with the period 1961–1990 (shown in blue) and the more recent period 2000–2009 (shown in red) for Austari-Jökulsá (vhm 144). Snow storage seasonality for each scenario for 2021–2050 is shown with grey broken curves and the area between maximum and minimum predicted snow storage is colored grey.
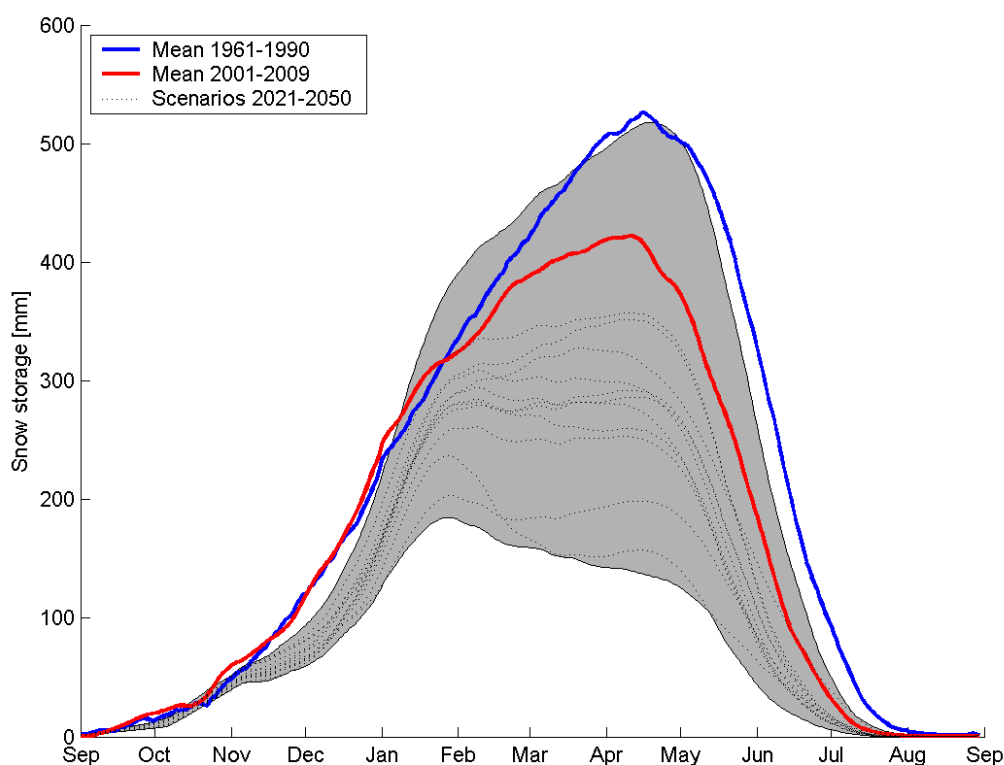
6 Discussion

Increased average winter discharge is found in the future simulations for both modelled watersheds, see Figure 6 and Figure 7. This increased average discharge may be formed by both increased base flow with relatively even discharge and/or from increased number of peaks. The predicted increase is a combined effect of both for the two watersheds. For Sandá í Þistilfirði, increased base flow is though not noted until the later part of the scenario period and the winter discharge increase therefore mainly originated from increased magnitude and number of melt peaks during winter. For Austari Jökuslá, the total amount of available water for runoff is increased because of both enhanced glacier melting and the predicted increase of precipitation. This causes higher water levels in soil and groundwater reservoirs which leads to higher base flow although increased magnitude and number of melt peaks is also a factor. Glacier melt is also extended into the autumn causing groundwater recharge over longer time period and with timing closer to the low discharge season, see Figure 8.

During the reference period 1961−1990, snow storage has a dominating effect on the discharge seasonality and snowmelt spring floods are the largest floods of the year for both watersheds, see Figure 6 and Figure 7. An important predicted change during winter

time is decreased snow storage, see Figure 11 and Figure 12. The causes are increased winter temperature causing more precipitation to fall as rain instead of snow and leading to increased melting of the snow cover during winter by increased magnitude and number of melt events. This decreased snow storage results is less snow being available for melt during spring causing decreased volume and diminished maximum discharge of spring floods.

Decreased spring floods are observed for both watersheds and all scenarios except one scenario for Austari-Jökulsá where snow storage is predicted to be largely unchanged (and thereby also the spring floods), see Figure 7 and Figure 12, because of a large precipitation increase and a small temperature increase, see further discussion below. The predicted shortening of time with considerable snow cover from 7 months to 3–5 months per year for approximately 2°C of warming is in the higher range of observed historical changes as increased temperature of 1°C has been observed to shorten the period of snow cover by 3–4 weeks (Björnsson *et al.*, 2008).

For Sandá í Þistilfirði the diminishing of spring floods affects the discharge during summer substantially as the spring melt peak was large and a dominant feature, see *Figure 6*. For Austari-Jökulsá an earlier onset of glacier melt and its increase in magnitude partly compensates for the effect of diminished spring floods during early summer and causes a large increase in discharge during the latter part of the summer when glacier discharge is dominant, see Figure 7 and Figure 8.

For Austari-Jökulsá the increase of glacier runoff and decrease of spring snow melt causes the glacier melt peak to become the main discharge peak during the year. The spring snow melt peak and the glacier melt peak do also become more detached. Similar detachment and change of relative magnitude of spring floods and the glacier originated maxima is seen in a comparison between the 25% warmest years and the 25% coldest years of historical discharge for Vestari-Jökulsá. Vestari-Jökulsá is adjacent to Austari-Jökulsá to the west and also drains part of Hofsjökull. These trends did, however, not become evident in a similar comparison of historical discharge for cold and warm years for Austari-Jökulsá (Philippe Crochet, personal communications). The 25% warmest years of the historical data are, however, colder than the predicted future temperatures for 2021–2050 so this study of historical data dose not exclude the predicted future changes.

For Austari-Jökulsá in 2021–2050, the occurrence of the highest discharge of the year is often moved from the spring melt peak in May, April or June to short-lived winter flood peaks in January, February, or March. The occurrence of the annual maximum discharge during the broad glacier peak in late summer is also predicted to become more common.

These changes become clearer by comparing the timing of the annual maximum discharge for the reference period 1961–1990 and the scenario period 2021–2050, see Figure 13. For the scenario period the average for all thirteen scenarios is shown in red while the maximum and minimum ratios for each month are given in grey. During the scenario period the annual maximum is located in the broad glacier peak for 13% of incidents on the average compared to 0% for the reference period. This is, however, quite different between scenarios. For the warmer scenarios this increase of glacier runoff is much larger and the glacier originated peak is predicted to become the highest annual discharge peak in up to 30% of all years in these scenarios.
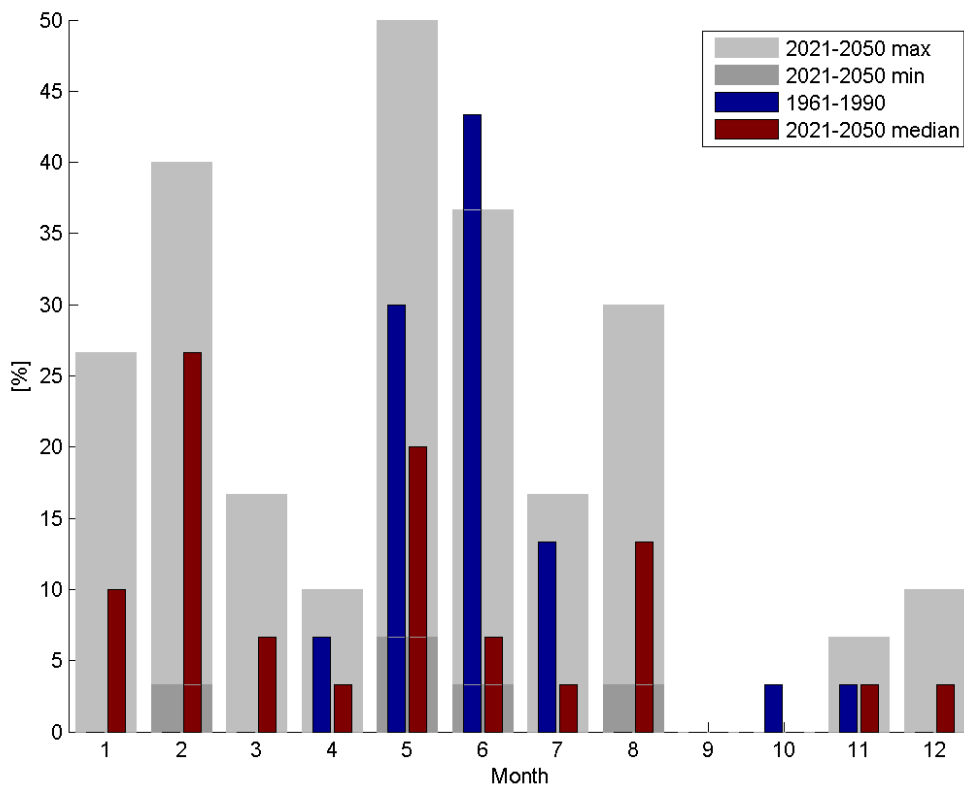
Figure 13. The ratio of the annual maximum discharge occurring in each month for the reference period and the average of the thirteen future scenarios, shown in red and blue columns respectively, for Austari-Jökulsá (vhm 144). The maximum and minimum number of events with respect to all thirteen different scenarios is shown in different shades of grey for each month.

A similar shift of the yearly maximum discharge from the spring melt peak to discrete shortlived winter events is found for Sandá í Þistilfirði, see Figure 14. The snow melt peak does, however, still hold its place as the most pronounced and voluminous discharge peak of the year, see Figure 6, although it is decreased by 45%−70% depended on climate scenario. The number of years with autumn and early winter floods, caused by large precipitation events being the largest annual flood, is also increased, see Figure 14.
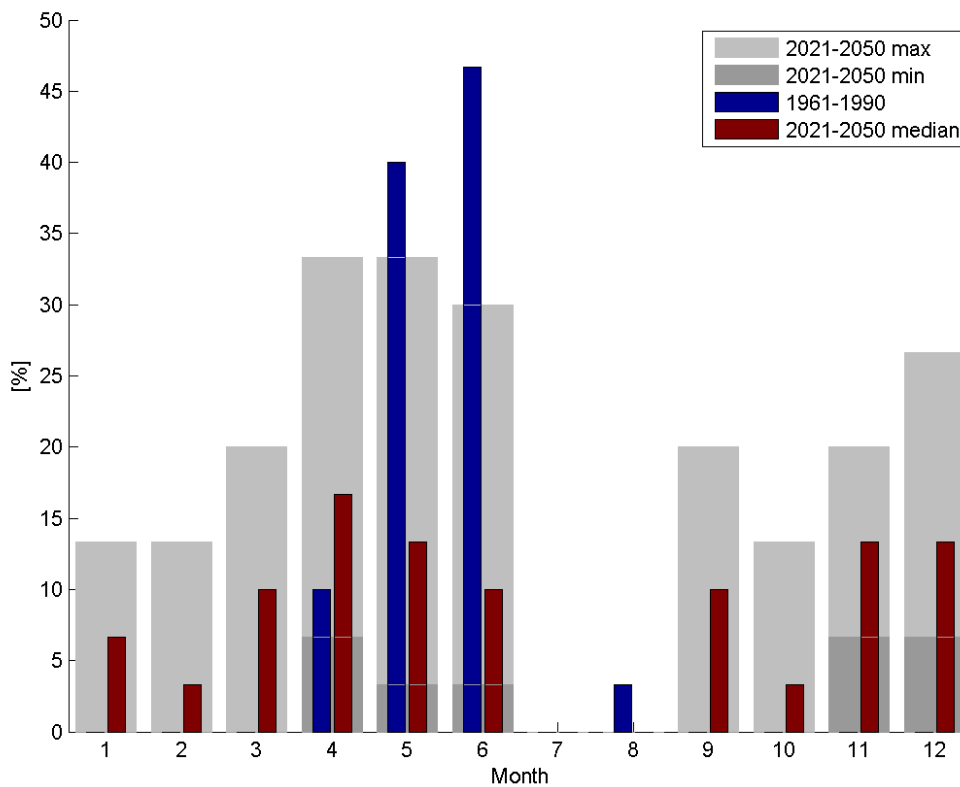
Figure 14. The ratio of the annual maximum discharge occurring in each month for the reference period and the average of the thirteen future scenarios, shown in red and blue columns respectively, for Sandá í Þistilfirði (vhm 26). The maximum and minimum number of events with respect to all thirteen different scenarios is shown in different shades of grey for each month.

Using monthly δ-changes to shift specific past years will cause daily temperature and precipitation changes to be dominated by the day to day temperature and precipitation of the particular chosen past year. The average of three past years is used to reduce this effect of the choice of year, but extreme events on time-scale of few days as precipitation floods and winter thaw floods will still be influenced by the selected past years. Any discussion of changes in flood size and changes in return period of floods it therefore unrealistic and will be affected by this methodology.

Changes of flood timing on a monthly scale can on the other hand be studied as specific δ-change for each future month origin from the internal variability of the climate scenarios is used. Results regarding changes in the timing of flood events can nevertheless still be affected by the monthly discharge variability of the three selected past years and should therefore been taken with precaution. The timing of the largest flood peak of each year is dominated by the main flood mechanisms of the watershed. The timing of annual maxima is different between rivers dominated by spring snow melt floods, autumn rain floods, or flash floods during wintertime caused by rain, snow melt, and frozen ground. The methodology used here should be able to catch such changes of the dominant flood mechanisms. The dominant flood mechanisms will also affect changes in the magnitude of the annual maxima.

In autumn, discharge is increased for Austari-Jökulsá, see Figure 7, because of longer extent of the glacier melt peak and increased precipitation as mentioned above. For Sandá í Þistilfirði autumn discharge is on the other hand not much changed, see Figure 6, as a significant precipitation increase is not predicted for this watershed. Changed snow regime does not affect autumn discharge as snow accumulation and melt does not occur in autumn during the reference period nor during the scenario period.

Evapotranspiration is predicted to be enhanced by 5–10% (depended on watershed and climate scenarios) for both of the watersheds discussed here. Evapotranspiration has a strong climatic connection and depends on temperature, vapour pressure, wind velocity, incoming radiation and other factors (Viessman & Lewis, 2003). Availability of water in the soil and on the surface of the watershed does also play a major role. Changes in evapotranspiration with changed climate and increased temperature are therefore complicated. The use of the simple Hamon evapotranspiration scheme is a drawback, but it is a simple empirical formulation building on temperature as an indicator of evapotranspiration. More physically based Penman-Monteith scheme will be used in future work.

The overall changes in runoff characteristics predicted by the different scenarios are similar, increased glacier melting for Austari-Jökulsá and decreased snow cover and spring floods for both watersheds. The magnitudes of changes are on the other hand different for the two watersheds and between the scenarios.

One scenario is an exception for Austari-Jökulsá with regard to diminished spring floods. The snow storage and spring melt are not much changed for this scenario, see Figure 7, Figure 10 and Figure 12. This scenario (MIUB_Echo_G) is relatively wet with 23% precipitation increase and it is the coldest one, but still 1.2°C warmer than the reference period on average. This large precipitation increase and small temperature increase compensate each other with regard to snow accumulation leaving the snow storage approximately unchanged. Earlier onset of glacier melt because of warming along with higher base flow because of increased precipitation causes an increase in the magnitude of total spring flow because they add to snow melt flood with undiminished magnitude.

The scenarios used in this study cover a wide range of climate projections, but they are not meant to cover the whole range of possible future climates. The future prediction of climate is and will be uncertain and thereby the hydrological prediction made above. There is also uncertainty inherent in the application of the δ-change method to prepare the climate scenario for use in hydrological modelling. There is also a certain amount of uncertainty in the hydrological modelling originated both from the physical representation of natural processes and in the parameterization of the model. Quantifying this uncertainty is hard as it origin is complicated and broad. As the true evolution of future climate is uncertain (IPCC, 2007) this can be assumed to be one of the largest contributors to the total uncertainty. The evolution of human society and greenhouse gas emissions is also highly uncertain but this is a relatively small contributing factor for the next few decades as most emission scenarios give similar results until the middle of 21st century (Björnsson *et al*., 2008). This uncertainty is not addressed here as all of the scenarios used here are based on the same greenhouse gas emission scenario, SRES A1B (IPCC, 2007; Kjellström, 2010).

Compared to the period 1961–1990 a warming of about 1°C has already been observed for the watersheds during the period 2000–2009, causing considerable discharge changes in the same direction as the predicted future changes.

7 Conclusions

The results presented here regarding increased glacier runoff, decreased snow cover and reduced spring floods are in line with former work done in the Climate and Energy project (Bergström *et al.*, 2007; Jónsdóttir, 2008) and "Veður og Orka" project (Jóhannesson *et al.*, 2007). The main improvements compared to earlier work is a better representation of physical hydrological processes in the hydrological modelling by using the groundwater module and the use of a suite of different climate scenarios to account for the effect of variability and uncertainties in predictions of future climate on the hydrological simulations. The use of monthly δ-change rather than one δ-changes for the whole period is also a major improvement. As mentioned above, the use of monthly δ-change preserves the monthly variability from the climate scenario and thereby variations between warm and cold periods and between wet and dry periods within the year. This was not the case for the methods employed in the former studies where only one δ-change value was used for the whole period as that does only reproduce the inter annual variability of the reference period for the future time period (Bergström *et al.* 2007).

8 Acknowledgments

References

Bergström, S., Jóhannesson, T., Aðalgeirsdóttir, G., Ahlstrøm, A., Andreassen, L. M., Andréasson, J., Beldring, S., Björnsson, H., Carlsson, B., Crochet, P., de Woul, M., Einarsson, B., Elvehøy, H., Flowers, G.E., Graham, L. P., Gröndal, G. O., Guðmundsson, S., Hellström, S.-S., Hock, R., Holmlund, P., Jónsdóttir, J. F., Pálsson, F., Radic, V., Reeh, N., Roald, L. A., Rosberg, J., Rogozova, S., Sigurðsson, O., Suomalainen, M., Thorsteinsson, Th., Vehviläinen, B. & Veijalainen, N. (2007). *Impacts of climate change on river runoff, glaciers and hydropower in the Nordic area. Joint final report from the CE Hydrological Models and Snow and Ice Groups.* Reykjavík: Climate and Energy. Report no. CE-6.

Björnsson, H., Sveinbjörnsdóttir, Á. E., Daníelsdóttir, A. K., Snorrason, Á., Sigurðsson, B. D., Sveinbjörnsson, E., Viggósson, G., Sigurjónsson, J., Baldursson, S., Þorvaldsdóttir, S. & Jónsson, T. (2008). *Hnattrænar loftslagsbreytingar og áhrif þeirra á Íslandi – Skýrsla vísindanefndar um loftslagsbreytingar.* Reykjavík: Umhverfisráðuneytið. (In Icelandic).

Crochet, P. & Jóhannesson, T. (2011). *Gridding daily temperature in Iceland.* (In preparation).

Döscher, R., Wyser, K., Markus Meier, H. E., Qian, M. & Redler, R. (2010). Quantifying Arctic contributions to climate predictability in a regional coupled ocean-ice-atmosphere model. *Climate Dynamics,* 34(7–8), 1157–1176.

Einarsson, B. & Jónsson, S. (2010). *Improving groundwater representation and the parameterization of glacial melting and evapotranspiration in applications of the WaSiM hydrological model within Iceland.* Reykjavík: Icelandic Meteorological Office, Report, 2010-017.

Fenger, J. (ed). (2007). *Impacts of Climate Change on Renewable Energy Sources. Their role in the Nordic energy system.* Copenhagen: Nordic Council of Ministers. Nord 2007:003, ISBN 978-92-893-1465-7, 192 pp.

Grell, G. A., Duhia, J. & Stauffer, D.R. (1994). *A description of the fifth generation Penn State/NCAR Mesoscale Model (MM5).* NCAR Tech. Note NCAR/TN398+STR, 138 pp.

Icelandic Meteorological Office (2010a). *Rennslisskýrsla vatnsárið 2008/2009, V433, Austari-Jökulsá, Skatastaðir.* Reykjavík: Icelandic Meteorological Office. (In Icelandic).

Icelandic Meteorological Office (2010b). *Rennslisskýrsla vatnsárið 2008/2009, V316, Sandá, Flögubrú II.* Reykjavík: Icelandic Meteorological Office. (In Icelandic).

IPCC. 2007. *Climate Change 2007: The Physical Science Basis. Contribution of Working Group I to the Fourth Assessment Report of the Intergovernmental Panel on Climate Change.* Solomon, S., Qin, D., Manning, M., Chen, Z., Marquis, M., Averyt, K. B., Tignor, M. & Miller, H. L. Jr. (*eds*). Cambridge, UK, and New York, NY, USA, Cambridge University Press, 996 pp.

Jasper, K., Gurtz, J. & Lang, H. (2002). Advanced flood forecasting in Alpine watersheds by coupling meteorological observations and forecasts with a distributed hydrological model. *Journal of Hydrology, 267*, 40–52.

Jasper, K. & Kaufmann, P. (2003). Coupled runoff simulations as validation tools for atmospheric models at the regional scale. *Quart. J. Roy. Meteor. Soc. 129*, 673–692.

Jóhannesson, T., Aðalgeirsdóttir, G., Björnsson, H., Crochet, P., Elíasson, E.B., Guðmundsson, S., Jónsdóttir, J. F., Ólafsson, H., Pálsson, F., Rögnvaldsson, Ó., Sigurðsson, O., Snorrason, Á., Blöndal Sveinsson, Ó. G. & Thorsteinsson, Th. (2007). *Effect of climate change on hydrology and hydro-resources in Iceland*. Reykjavík: National Energy Authority–Hydrological Service. OS-2007/011, ISBN: 978-9979-68-224-0.

Jóhannesson, T. 2010. *Sviðsmyndir um loftslagsbreytingar á Íslandi fyrir jökla- og vatnafræðilega líkanreikninga í CES og LOKS verkefnunum*. Reykjavík: Veðurstofa Íslands, Memo-TóJ-2010-02. (In Icelandic).

Jónsdóttir, J. F. (2008). A runoff map based on numerically simulated precipitation and a projection of future runoff in Iceland. *Hydrological Sciences Journal, 53(1)*, 100–111.

Kjellström, E. (2010). *Deliverable 4.3: Report on user dialogue and analysis of regional climate scenarios for northern Europe.* The CES-project, technical report, final version delivered 15 April 2010.

Kunstmann, H., Krause, J. & Mayr, S. (2006). Inverse distributed hydrological modelling of Alpine catchments. *Hydrol. Earth Syst. Sci., 10*, 395–412.

Nawri, N. & Björnsson, H. (2010). *Surface air temperature and precipitation trends for Iceland in the 21st century.* Reykjavík: Icelandic Meteorological Office, Report, 2010-005.

Rist, S. (1990). *Vatns er þörf.* Reykjavík: Bókaútgáfa Menningarsjóðs. (In Icelandic).

Rögnvaldsson, Ó., Jónsdóttir, J. F. & Ólafsson, H. (2007). Numerical simulation of precipitation in the complex terrain of Iceland – Comparison with glaciological and hydrological data. *Meteorologische Zeitschrift,* 16(1), 71–85.

Schulla, J. & Jasper, K. (2007). *Model Description WaSiM-ETH (Water balance Simulation Model ETH).* Retrieved from http://wasim.ch/downloads/doku/wasim/ wasim_2007_en.pdf

Snorrason, Á. & Harðardóttir, J. (2008). Climate and Energy Systems (CES) 2007–2010. A new Nordic energy research project. [Extended abstract]. *Northern hydrology and its global role: XXV Nordic hydrological conference, Nordic Association for Hydrology, Reykjavík, Iceland August 11–13.* Reykjavík: Icelandic Hydrological Committee, 591–596.

Viessman, Jr. W. & Lewis, G. L. (2003). *Introduction to Hydrology, Fifth Edition*, New Jersey: Pearson Education, Inc.